Electronic Supplementary Material (ESI) for Physical Chemistry Chemical Physics.

Supplementary Information

Functional Porous Carbon-ZnO Nanocomposites for the High-Performance Biosensors and Energy Storage Applications

Rajesh Madhu,[*a,b†] Vediyappan Veeramani,[b†] Shen-Ming Chen,[*b] Pitchaimani Veerakumar[c†] Shang-Bin Liu[*cd] and Nobuyoshi Miyamoto,[a]

[a] Department of Life, Environment, and Materials Science, Fukuoka Institute of Technology, 3-30-1, Wajirohigashi, Higashiku, Fukuoka 811-0295, Japan.

[b] Department of Chemical Engineering and Biotechnology, National Taipei University of Technology, Taipei 10608, Taiwan.

[c] Institute of Atomic and Molecular Sciences, Academia Sinica, Taipei 10617, Taiwan.

[d] Department of Chemistry, National Taiwan Normal University, Taipei 11677, Taiwan.

* Corresponding authors:

E-mails: rajesphysics@gmail.com (R. Madhu); smchen78@ms15.hinet.net (S. M. Chen; Tel: +886-2-2701 7147; Fax: +886-2-270 2523); sbliu@sinica.edu.tw (S. B. Liu; Tel: +886-2-2366 8230; Fax: +886-2-2362 0200).

****

Ash content calculation

2.0 g of bagasse placed in a pre-weighted crucible was incinerated in a muffle furnace was heated until complete ashing was achieved. The crucible was cooled to room temperature and reweighed. Ash content was calculated between the differences in weight of the crucible by using the equation:[S1]

$$\text{ash content (wt\%)} = (W_2 - W_0)/(W_1 - W_0) \times 100\ \%,$$

where W_0 = weight of the crucible, and W_1 and W_2 represent total weight (crucible + sample) before and after the incineration treatment, respectively. Accordingly, the amount of ash content of 10.31 wt% was attained from the washed and incinerated sugarcane powder.

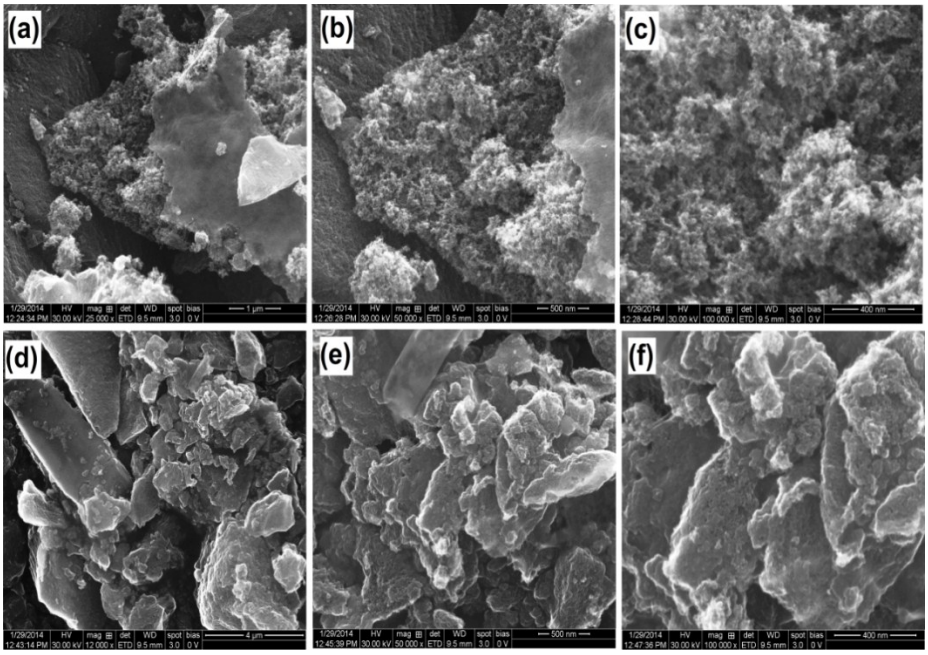

Fig. S1 FE-SEM images of the calcined (900 °C) (a–c) ZAC-10 and (d–f) ZAC-20 samples with different magnifications.

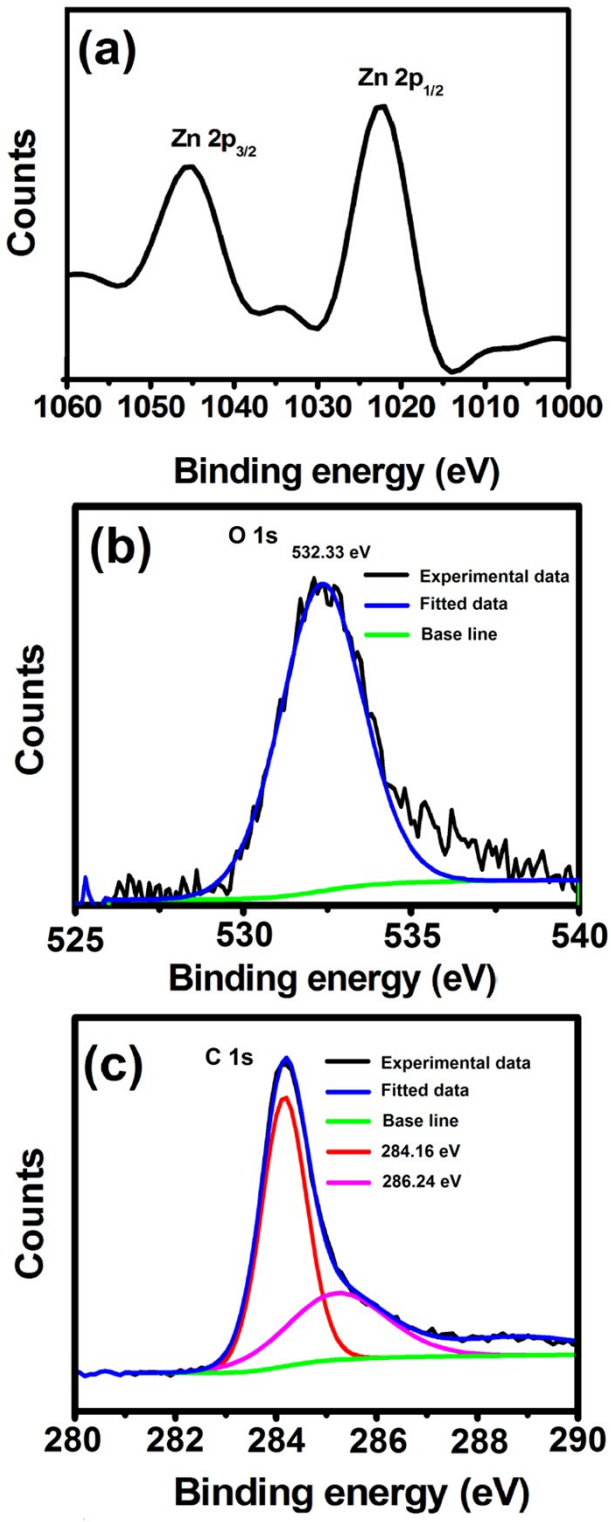

Fig. S2 Expanded XPS profiles in the (a) Zn 2p, (b) O 1s, and (c) C 1s regions of the ZAC-20 sample.

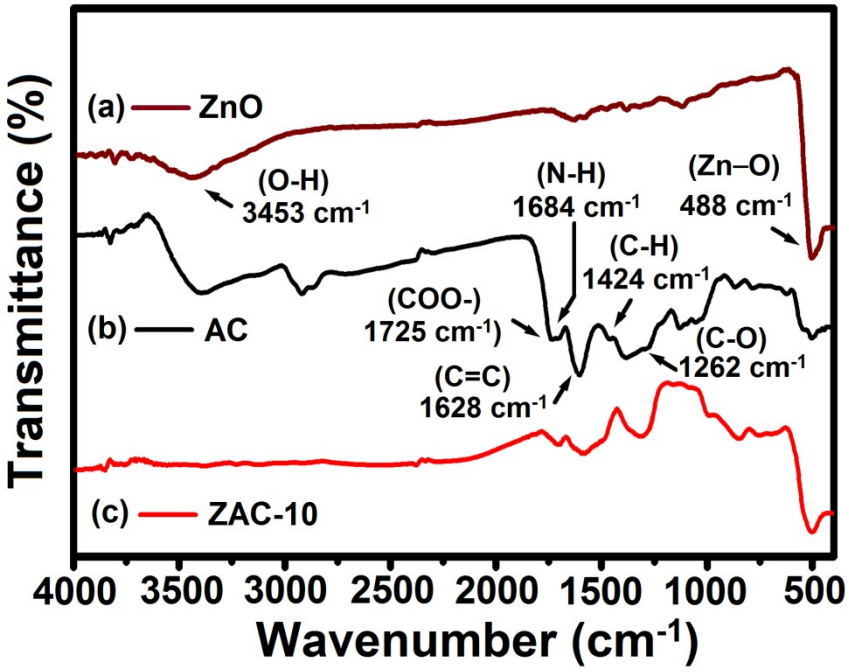

Fig. S3 FT-IR spectra of the (a) ZnO (b) AC, and (c) ZAC-10 samples.

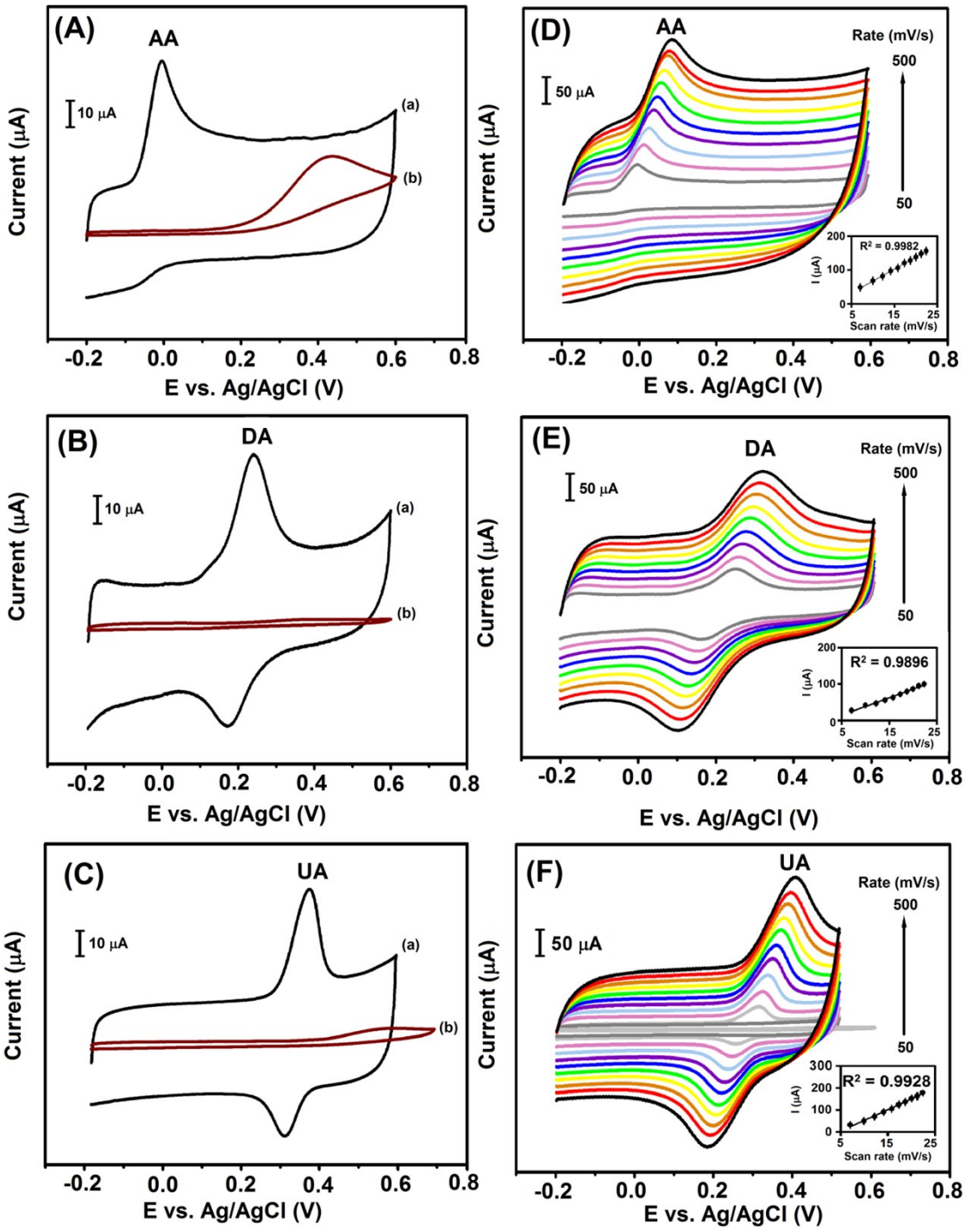

Fig. S4 CV curves of (a) ZAC-20 modified and (b) bare GCEs in 0.1 M PBS (pH = 7.0) with (A) 50 μM AA, (B) 10 μM DA, (C) 10 μM UA recorded at a constant (50 mV s^{-1}) and (D)–(F) varied scan rates (50–500 mV s^{-1}), respectively. Insets: calibration plots of anodic peak current *vs* scan rate.

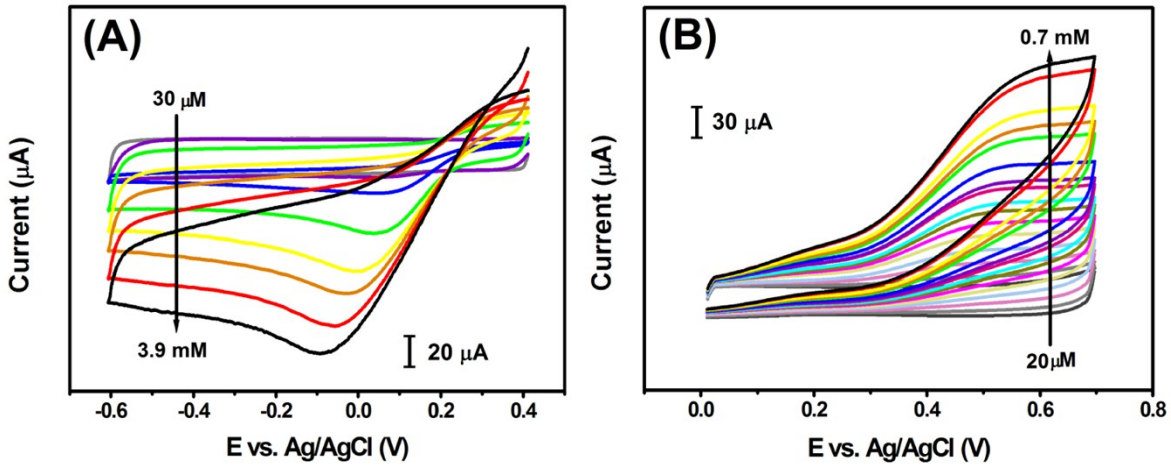

Fig. S5 CV curves of the ZAC-20 modified GCE in 0.1 M PBS (pH = 7.0) with varied concentrations of (A) H_2O_2 (30 μM to 3.9 mM) and (B) N_2H_4 (20 μM to 0.7 mM). All measurements were conducted with a scan rate of 50 mV s^{-1}.

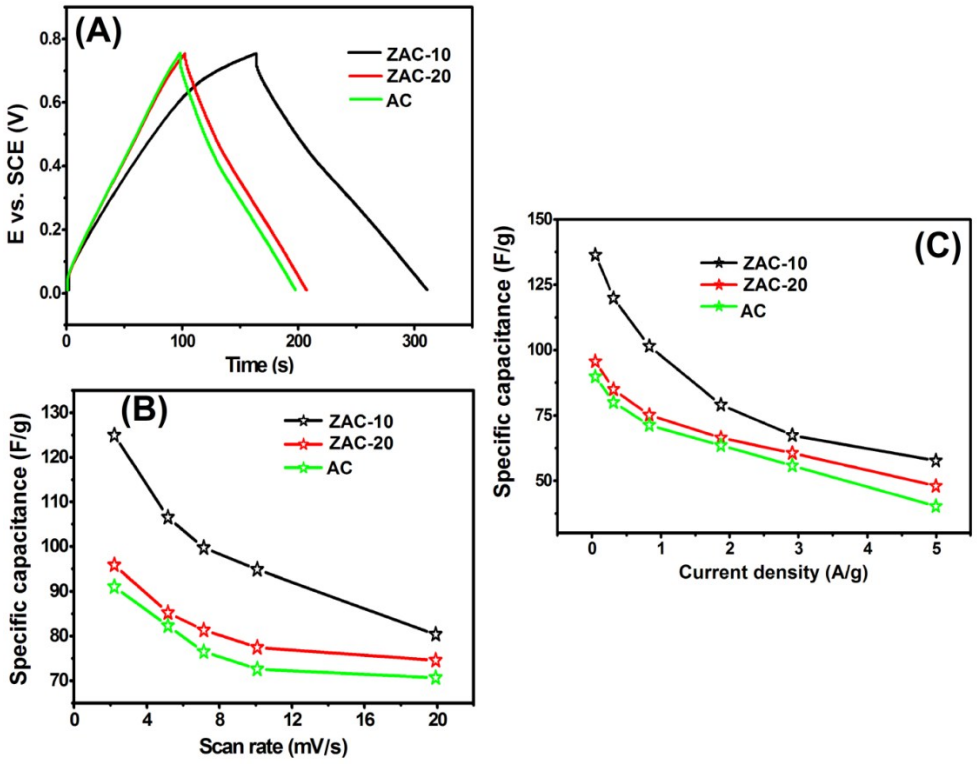

Fig. S6 (A) GCD curves, (B) specific capacitance *vs* scan rate, and (C) specific capacitance *vs* current density, obtained from various AC, ZAC-10, and ZAC-20 modified electrodes.

Table S1 Comparison of analytical parameters for simultaneous detection of AA, UA, and DA over various modified electrodes*

Working electrode	Potential difference (mV)			Linear range (μM)			Detection limit (nM)			Ref.
	AA■DA	DA■UA	UA■AA	AA	DA	UA	AA	DA	UA	
MCNF-modified pyrolytic GCE	223	149	382	0.1–10	0.05–30	0.5–120	50000	20	200	[S1]
ZnO NWA-graphene foam	60	100	210	0–80	0-40	0–40	100	10	20	[S2]
NDPC nanopolyhedra/GCE	228	124	352	80–2000	0.5–30	4–50	740	11	21	[S3]
HNDC spheres-RGO/GCE	252	132	384	50–1200	0.5–90	1–70	650	12	18	[S4]
C_{60} hollow microspheres/GE	280	80	200	1–13	0.01–2	10–100	1000	0.12	1000	[S5]
NID nanowire/Si substrates	286	138	304	---	0.5–10	---	---	360	---	[S6]
CTAB-f-GO-MWCNTs/GCE	210	90	300	5.0–300	5.0–500	3.0–60	1000	1500	1000	[S7]
CFE modified by GF/ CFE	110	100	210	74–2305	1–126	4–371	24700	500	2000	[S8]
PtNPs-RGO/GCE	---	163	---	---	10–170	10–130	---	250	450	[S9]
ZAC-20/GCE	175	144	319	1.9–38.40	0.5–15.74	0.5–15.75	123	8	12	This work

*MCNF = mesoporous carbon nanofiber; GCE = Glassy carbon electrode; ZnO-NWA = zinc oxide nanowire array; NDPC = nitrogen-doped porous carbon; HNDC = hollow nitrogen doped carbon; RGO = reduced graphene oxide; GE = gold electrode; NID = nitrogen incorporated diamond; CTAB-f-GO = cetyltrimethylammonium bromide-functionalized graphene oxide; MWCNTs = multi-walled carbon nanotubes; GF = graphene flowers; CFE = carbon fiber electrode; PtNPs = platinum nanoparticles; ZAC-20 = 20 wt% ZnO-AC nanocomposite.

Table S2 Comparison of analytical parameters for detection of H_2O_2 over various modified electrodes*

Working electrode	Potential (V)	Technique	Sensitivity (μA/μM·cm^2)	Detection limit (μM)	Linear range (μM)	pH	Ref.
PBNPs-(3D-CGF-MC-KS)/INCE	–0.05	Amperometry	78.64	0.10	1–21750	6.0	[S10]
Au−Cu_x OS yolk−shell nanostructures/GCE	–0.20	Amperometry	50.41	0.01	0.01–5.12	7.4	[S11]
Au-RGO/GPE	0.10	Magnetic stirring	236.80	2.00	5–8600	7.4	[S12]
CuS-RGO/GCE	–0.27	Amperometry	0.03	0.27	5–1500	7.4	[S13]
N-DGE/GCE	–0.59	CV	---	---	0.01–5000	7.0	[S14]
IrO_2-Pt-ME	0.20	Amperometry	---	---	0–1000	7.4	[S15]
MnO_2 ultrathin nanosheets	0.70	Amperometry	130.56	1.50	5–3500	7.0	[S16]
PNEGHNs/GCE	0.0	Amperometry	---	0.08	1–500	7.0	[S17]
ZAC-20/GCE	0.05	Amperometry	0.62	1.93	99–2439	7.0	This work

*PBNPs = Prussian blue nanoparticles; 3D-(CGF-MC-KS) = three-dimensional carboxylic group-functionalized macroporous carbon derived from kenaf stem; INCE = inorganic nanocomposite electrode; Cu_xOS = copper sulfate nanoparticles; GCE = glassy carbon electrode; Au-RGO = gold nanoparticles decorated on reduced graphene oxide; GPE = graphene paper electrode; CuS = copper sulfide; N-DGE = nitrogen-doped graphene electrode; CV = cyclic voltammetry; IrO_2 = iridium dioxide; Pt-ME = platinum microelectrode; MnO_2 = manganese dioxide; PNEGHNs = nanoparticle ensemble-on-graphene hybrid nanosheet; ZAC-20 = 20 wt% ZnO-AC nanocomposite.

Table S3 Comparison of analytical parameters for detection of hydrazine over various modified electrodes*

Working electrode	Technique	Sensitivity (μA/μM·cm²)	Detection limit (μM)	Linear range (μM)	pH	Ref.
CeO_2-OMC/GCE	Amperometry	0.15	0.01	0.04–192	8.0	[S18]
HPIMBD-MWCNT/GCE	Amperometry	0.02	1.10	4.0–32.9 32.9–750.4	7.0	[S19]
PVP-AgNCs/GCE	Amperometry	---	1.10	5–460	7.4	[S20]
ZnO/GE	Amperometry	97.13	0.15	0.1–1	7.0	[S21]
CuS-RGO/GCE	Amperometry	0.82	0.30	1–1000	7.0	[S22]
ZnO/Au	Amperometry	1.60	0.07	0.07–415	7.4	[S23]
QZMNCPE/GCE	DPV		0.08	0.5– 1900	7.0	[S24]
PCF/GCE	Amperometry	0.21	0.14	1–550	7.5	[S25]
ZnO/MWCNT/GCE	Amperometry	0.25	0.18	0.6–250	7.4	[S26]
ZnO-RGO (4.4 : 1)	Amperometry	---	0.8	1–33.5	13	[S27]
ZAC-20/GCE	Amperometry	10	0.03	0.19–19.8 207–303	7.0	This work

*CeO_2 = cerium oxide; OMC = ordered mesoporous carbon; GCE = glassy carbon electrode; HPIMBD = 4-((2-hydroxyphenylimino)methyl)benzene-1,2-diol; MWCNT = multi-walled carbon nanotube; PVP = poly(vinylpyrrolidone); AgNCs = silver nanocubes; ZnO = zinc oxide; GE = gold electrode, CuS = copper sulfide; RGO = reduced graphene oxide, QZMNCPE = quinizarine-modified TiO_2 nanoparticles carbon paste electrode; PCF = pyrolytic carbon film; ZAC-20 = 20 wt% ZnO-AC nanocomposite.

References

(S1)_ Y. Yue, G. Hu, M. Zheng, Y. Guo, J. Cao and S. Shao, *Carbon*, 2012, **50**, 107–114.

(S2) H. Y. Yue, S. Huang, J. Chang, C. Heo, F. Yao, S. Adhikari, F. Gunes, L. C. Liu, T. H. Lee, E. S. Oh, B. Li, J. J. Zhang, T. Q. Huy, N. V. Luan and Lee, Y. H. *ACS Nano*, 2014, **8**, 1639–1646.

(S3) P. Gai, H. Zhang, Y. Zhang, W. Liu, G. Zhu, X. Zhang and J. Chen, *J. Mater. Chem. B*, 2013, **1**, 2742–2749.

(S4) H. Zhang, P. Gai, R. Cheng, L. Wu, X. Zhang and J. Chen, *Anal. Methods*, 2013, **5**, 3591–3600.

(S5) L. Wei, Y. Lei, H. Fu and J. Yao, *ACS Appl. Mater. Interfaces*, 201**2**, **4**, 1594−1600.

(S6) J. Shalini, K. J. Sankaran, C.-Li. Dong, C.-Y. Lee, N.-H. Tai and I.-N. Lin, *Nanoscale*, 2013, **5,** 1159–1167.

(S7) Y. J. Yanga and W. Li, *Biosens. Bioelectron.*, 2014, **56**, 300–306.

(S8) J. Du, R. Yue, F. Ren, Z. Yao, F. Jiang, P. Yang and Y. Du, *Biosens. Bioelectron.*, 2014, **53**, 220–224.

(S9) T. Q. Xu, Q. L. Zhang, J. N. Zheng, Z. Y. Lv, J. Wei, A. J. Wang and J. J. Feng, *Electrochim. Acta*, 2014, **115**, 109–115.

(S10) L. Wang, Q. Zhang, S. Chen, F. Xu, S. Chen, J. Jia, H. Tan, H. Hou and Y. Song, *Anal. Chem*., 2014, **86**, 1414−1421.

(S11) L. Zhou, L. Kuai, W. Li and B. Geng, *ACS Appl. Mater. Interfaces*, 2012, **4**, 6463−6467.

(S12) F. Xiao, J. Song, H. Gao, X. Zan, R. Xu and H. Duan, *ACS Nano*, 2012, **6**, 100–110.

(S13) J. Bai and X. Jiang, *Anal. Chem.*, 2013, **85**, 8095−8101.

(S14) Y. Wang, Y. Shao, D. W. Matson, J. Li and Y. Lin, *ACS Nano*, 2010, **4**, 1790–1798.

(S15) J. H. Shim, Y. Lee, M. Kang, J. Lee, J. M. Baik, Y. Lee, C. Lee and M. H. Kim, *Anal. Chem.*, 2012, **84**, 3827−3832.

(S16) P. Zhang, D. Guo and Q. Li, *Mater. Lett.*, 2014, **125**, 202–205.

(S17) S. Guo, D. Wen, Y. Zhai, S. Dong and E. Wang, *ACS Nano*, 2010, **4**, 3959–3968.

(S18) Y. Liu, Y. Li and X. He, *Analytica Chimica Acta*, 2014, **819**, 26–33.

(S19) R. Devasenathipathy, V. Mani and S. M. Chen, *Talanta*, 2014, **124**, 43–51.

(S20) Y. Wanga, X. Yanga, J. Bai, X. Jianga, G. Fan, *Biosens. Bioelectron.*, 2013, **43**, 180–185.

(S21) S. K. Mehta, K. Singh, A. Umar, G. R. Chaudhary, S. Singh, *Electrochim. Acta*, 2012, **69**, 128–133.

(S22) Y. J. Yanga, W. Li, X. Wu, *Electrochim. Acta*, 2014, **123**, 260–267.

(S23) W. Sultana, S. Ghosh, Eraiah, B. *Electroanalysis*, 2012, **24**, 1869–1877.

(S24) M. M. Ardakani, Z. Taleat, H. Beitollahi and H. Naeimi, *Nanoscale* 2011, **3**, 1683–1689.

(S25) M. Hadi, A. Rouhollahia and M. Yousefi, *Sensor. Actuat. B.*, 2011, **160**, 121–128.

(S26) B. Fang, C. Zhang, W. Zhang and G. Wang, *Electrochim. Acta*, 2009, **55**, 178–182.

(S27) J. Ding, S. Zhu, T. Zhu, W. Sun, Q. Li, G. Wei and Z. Su, *RSC Adv.*, 2015, **5**, 22935–22942.